Selected Paper

Theoretical Design of Monofunctional Psoralen Compounds in Photochemotherapy

Ayako Nakata, Takeshi Baba, and Hiromi Nakai*

Department of Chemistry, School of Science and Engineering, Waseda University, 3-4-1 Okubo, Shinjuku-ku, Tokyo 169-8555

Received December 14, 2006; E-mail: nakai@waseda.jp

The geometries and electronic structures in the lowest triplet (T_1) states of psoralen, 5-methoxypsoralen (5-MOP), 8-methoxypsoralen (8-MOP), and their monoadducts were studied by performing density functional theory (DFT) calculations. It was shown that the pyrone ring of 8-MOP is cleaved in the T_1 state and the cleaved pyrone ring loses the ability to bond to the thymine residue. Therefore, 8-MOP in the open-ring structure does not form a diadduct, which is thought to cause side effects. DFT calculations on 20 kinds of substituted psoralens showed that the cleavage of the pyrone ring in the T_1 state can be controlled by substituting an electron-donating group, especially one having a strong electron-donating resonance effect, at the 8-position of psoralen.

Psoralen (7*H*-furo[3,2-*g*][1]benzopyran-7-one) compounds, which are illustrated in Fig. 1, are a class of drugs used in the photochemotherapy of dermatologic diseases, such as psoriasis and vitiligo. The main reaction involved in the phototherapy is the photocycloaddition between psoralens and thymine residues in DNA.[1] The psoralens first insert themselves between adjacent thymine pairs in the DNA duplex. Upon irradiation with UV-A light (300–400 nm), a two-step photoreaction occurs producing monoadducts and diadducts as shown in Scheme 1. However, diadduct cross-linking between two strands of DNA sometimes causes side effects.[1–3] Therefore, the development of monofunctional psoralen compounds is greatly desired.

A psoralen compound has two photoreactive sites, namely the C4′–C5′ double bond in the furan ring and the C3–C4 double bond in the pyrone ring. Therefore, there are two kinds of monoadducts: furan and pyrone monoadducts.[1–3] It is assumed that the C4′–C5′ and C3–C4 bonds react via the first singlet excited (S_1) state and the lowest triplet (T_1) state, respectively.[1,2]

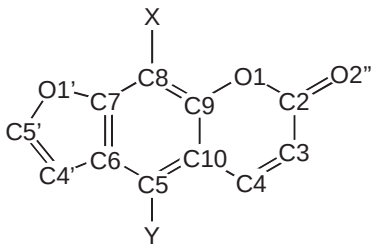

(X,Y) = (H, H) : Psoralen
(H, OCH_3) : 5-MOP
(OCH_3, H) : 8-MOP

Fig. 1. Chemical structure of isolated psoralen compound. The numbering in this figure (O1, C2, O2″, C3, C4, C5, C6, C7, C8, C9, C10, O1′, C4′, and C5′) corresponds to IUPAC numbering (O8, C7, O7′, C6, C5, C4, C3a, C9a, C9, C8a, C4a, O1, C2, and C3).

The transition absorption spectrum and the resonance Raman spectrum of psoralen, 5-methoxypsoralen (5-MOP), and 8-methoxypsoralen (8-MOP) have shown that the T_1 transient species of 8-MOP are quenched significantly more rapidly than those of psoralen and 5-MOP.[4] However, the reason for the specific behavior of 8-MOP has not been clarified by experimental approaches. Our previous ab initio molecular dynamics simulations have shown that the O1–C2 bond of 8-MOP cleaves in the T_1 state,[5] which is thought to be a reason of the specificity of 8-MOP. Although several theoretical studies for psoralen compounds have been reported[6–10] and the triplet excited states of psoralen have been investigated in detail,[11,12] the specificity of 8-MOP has not been discussed.

The aim of the present study was to clarify the differences of the electronic structures between psoralen, 5-MOP, and 8-MOP in the T_1 states in the isolated and furan monoadduct systems by performing density functional theory (DFT) calculations. Because pyrone monoadducts are reported not to form diadducts,[13–15] only furan monoadducts were investigated in this study. In the next section, the computational details of the present calculations are described. In the third section, the calculated geometries and spin densities in isolated and furan monoadduct systems are discussed. Then, monofunctional psoralen compounds, which do not lead to a harmful diadduct, are proposed. The last section gives the conclusion of this study.

Computational Details

Electronic structures of psoralen compounds in the singlet ground (S_0) and T_1 states were examined by DFT calculations at the B3LYP[16–21]/cc-pVDZ[22] level. We investigated singlet excitation energies of psoralens within the same computational level as our previous study,[13] in which the errors of calculated excitation energies of isolated psoralens from experimental data are at most 0.5 eV. With respect to the experimental S_1 excitation energy of psoralen, 3.73 eV,[23] the calculated one with B3LYP/cc-pVDZ[13] is 3.77 eV, while those with CASPT2/

Published on the web July 11, 2007; doi:10.1246/bcsj.80.1341

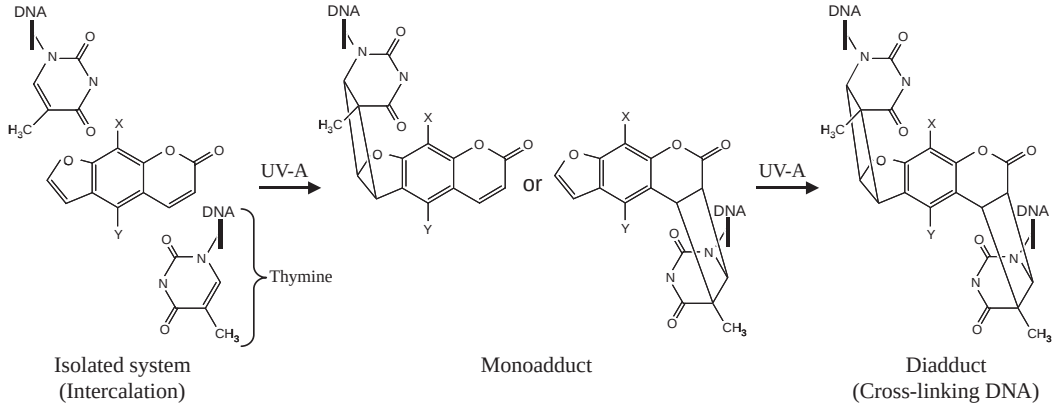

Scheme 1. Photoreaction scheme of psoralen compound to thymine residue.

ANO-L[6] and DFT/MRCI/TZVP+Ryd[7] are 3.98 and 3.81 eV, respectively. Therefore, B3LYP/cc-pVDZ method is thought to be accurate enough to describe excited states of psoralens. We investigated non-substituted psoralen, 5-MOP, and 8-MOP in isolated systems and their furan monoadducts. Twenty kinds of substituted psoralen compounds were also investigated. All of the geometrical parameters of the psoralen compounds in both the S_0 and T_1 states were optimized. All calculations were performed using Gaussian 03.[24]

Results and Discussion

Electronic Structures of Isolated Psoralens in the T_1 States. Figure 2 shows the energy diagrams of psoralen compounds in the S_0 and T_1 states. The vertical excitation energies from the S_0 to T_1 states of psoralen, 5-MOP, and 8-MOP at the ground-state structures were 3.00, 2.98, and 2.99 eV, respectively, which are similar to each other.

For psoralen and 5-MOP, two kinds of stable structure were obtained in the T_1 state, namely closed- and open-ring structures. The pyrone ring is cleaved in the open-ring structure, whereas the pyrone ring remains in the closed-ring structure. The closed-ring structure was more stable than the open-ring structure: for psoralen and 5-MOP, the stabilization energies, which correspond to the energy differences from the T_1-state energies of the ground-state structures, were 0.37 and 0.40 eV (8.62 and 9.16 kcal mol^{-1}) in the closed-ring structures and 0.24 and 0.13 eV (5.63 and 3.04 kcal mol^{-1}) in the open-ring structures, respectively. Transition states were obtained between the closed-ring and open-ring structures, which had barrier heights with respect to the closed-ring structures of 0.16 and 0.30 eV (3.78 and 6.98 kcal mol^{-1}) for psoralen and 5-MOP, respectively.

On the other hand, only the open-ring structure was obtained as the stationary point in the T_1 state for 8-MOP. Our previous AIMD simulation has demonstrated that 8-MOP can not keep the closed-ring form and changes to an open-ring structure immediately in the T_1 state.[5] The stabilization energy of the open-ring structure was 0.48 eV (10.98 kcal mol^{-1}), which is larger than those of psoralen and 5-MOP. Furthermore, no transition state was found between the ground-state structure and the open-ring structure, suggesting, therefore, that 8-MOP is more likely to form the open-ring structure than psoralen and 5-MOP.

The optimized bond distances in the ground-state structures and the closed- and open-ring structures in the T_1 states are summarized in Table 1. For the closed- and open-ring structures in the T_1 states, the differences from the ground-state structures are shown in parentheses. As for the closed-ring structures in the T_1 states, the C3–C4 bonds in psoralen and 5-MOP were elongated by more than 0.1 Å. The C10–C9 and C10–C5 bonds were also elongated by about 0.04 Å. The bond lengths of C3–C4, C10–C9, and C10–C5 were about 1.46 Å, which correspond to the C–C single bonds. The changes in the bonds in the furan rings were small: the changes in the C4′–C5′ bonds were 0.001 and 0.003 Å for psoralen and 5-MOP, respectively.

As regards the open-ring structure, the O1–C2 bond in pyrone ring was cleaved: the O1–C2 distances in psoralen (2.219 Å), 5-MOP (2.222 Å), and 8-MOP (2.215 Å) are significantly longer than those in the closed-ring structures. The C2–C3 and C9–O1 bonds were shortened by more than 0.1 Å, which indicates that those bonds become double bond-like. The C4–C10 and C2–O2″ bonds were shortened by about 0.02 and 0.04 Å, respectively. The elongations of the C3–C4 bonds were about 0.065 Å, which are smaller than those in the closed-ring structures. The C4′–C5′ bonds in the open-ring structures were elongated by about 0.2 Å. The C4′–C5′ bonds were more elongated in the open-ring structure than in the closed-ring structure.

Table 2 shows the spin distributions in psoralen compounds in the T_1 state in three different geometries, namely the ground-state structure and the closed- and open-ring structures obtained in the T_1 state. As for the ground-state structure, psoralen and 5-MOP had the largest amplitude at the C3 and C4 atoms: 0.536 and 0.369 in psoralen and 0.487 and 0.215 in 5-MOP, respectively, which indicates that C3 and C4 are reactive sites. The spin densities at C4′ and C5′, which are also thought to be photoreactive sites, were less than 0.1 in psoralen and 5-MOP. On the other hand, the spin densities at the C3 and C4 atoms in 8-MOP, which were 0.167 and 0.093, are smaller than those in psoralen and 5-MOP. It indicates that the C3 and C4 sites are not reactive in 8-MOP. On the other hand, the spin densities at C4′ and C5′ were 0.076 and 0.200, which are larger than those in psoralen and 5-MOP. Therefore, the C4′–C5′ sites in 8-MOP are more reactive than those in psoralen and 5-MOP.

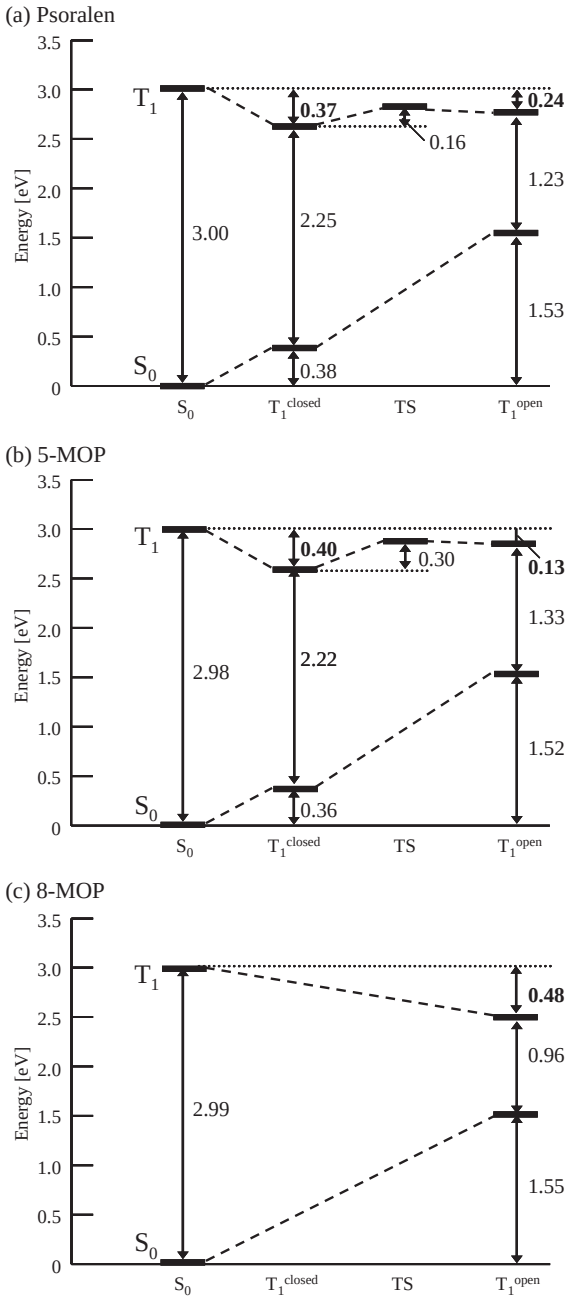

Fig. 2. Energy diagrams in the S_0 and T_1 states for isolated (a) psoralen, (b) 5-MOP, and (c) 8-MOP. Stabilization energies from the T_1-state energies at the ground-state structures are shown in boldface.

For the closed-ring structure obtained in the T_1 state, the spin densities at C3 and C4 increased to 0.638 and 0.414 in psoralen and to 0.665 and 0.383 in 5-MOP, which are larger than those in the ground-state structure. Thus, the structural relaxation after the excitation to the T_1 state makes the C3–C4 bond more single bond-like and reactive.

As for the open-ring structure, the absolute spin densities at C3 were at most 0.025, whereas those at C4 were about 0.5, which suggests that the cleavage of the O1–C2 bond critically decreases the activity at C3–C4 sites. The C4′–C5′ sites are slightly activated: the spin densities of C5′ were larger than those in the closed-ring structures.

The changes in the bond lengths and the spin distribution indicate that the bonds alternate in the closed- and open-ring structures in the T_1 states as shown in Fig. 3. The C3–C4 bond in the closed-ring structure is activated while that in the open-ring structure is not, which suggests that the cycloaddition to the C3–C4 sites in the pyrone ring does not occur when psoralens have the open-ring structure.

The high stability of the open-ring structure of 8-MOP in the T_1 state is thought to be due to a three-center bond among C2–O1–$O_{methoxy}$ atoms. In the open-ring structure of 8-MOP, the C2–O1 and O1–$O_{methoxy}$ distances were 2.215 and 2.629 Å, and the C2–O1–$O_{methoxy}$ angle was quasi-linear, 175.6°, which suggests the existence of the three-center bond. In Table 3, the stabilization energies of the closed- and open-ring structures against the T_1-state energies of the ground-state geometries are shown for 5-MOP and 8-MOP isomers, in which the methoxy groups are rotated and the lone-pair orbitals of $O_{methoxy}$ are out of the psoralen planes. Both closed- and open-ring structures were obtained for the isomers. The stabilization energies of the closed- and open-ring structures of the 8-MOP isomer are comparable to each other: 0.39 and 0.38 eV (8.90 and 8.67 kcal mol^{-1}), respectively. This means that the lone-pair orbital of $O_{methoxy}$ plays an important role in stabilizing the open-ring structure of 8-MOP. However, no explicit evidence has been provided by the analyses of the Kohn–Sham orbitals or the natural bond orbitals.

Electronic Structures of Furan Monoadducts in the T_1 States. There are two kinds of monoadducts, furan and pyrone monoadducts, as shown in Fig. 4. Since it has been reported that pyrone monoadducts do not lead to diadducts, we focused only on the furan monoadducts in this section. Figure 5 shows the energy diagrams of the furan monoadducts of psoralen compounds. The rigorous transition state of the furan monoadduct of 8-MOP could not be found so that the barrier height of the furan monoadduct of 8-MOP was estimated from the potential energy surface calculated by changing the O1–C2 distances at intervals of 0.005 Å.

For the furan monoadducts of psoralen and 5-MOP, both the closed- and open-ring structures were obtained. However, the open-ring structures were 0.16 eV (3.59 kcal mol^{-1}) less stable than the T_1-state energies at the ground-state structure, whereas the closed-ring structures were 0.35 eV (8.05 kcal mol^{-1}) more stable. The transition states with the barrier heights of 0.51 and 0.63 eV (11.77 and 14.50 kcal mol^{-1}) were obtained for psoralen and 5-MOP, respectively.

For 8-MOP, both the closed- and open-ring structures were obtained in the case of the furan monoadduct, whereas no stable closed-ring structure was found for the isolated system. The open-ring structure of 8-MOP was not destabilized, although those of psoralen and 5-MOP were highly destabilized: the stabilization energies of closed- and open-ring structures of 8-MOP were 0.36 and 0.19 eV (8.20 and 4.35 kcal mol^{-1}), respectively. Not only for the isolated system but also for the furan monoadduct, 8-MOP is suggested to be more likely to form the open-ring structure than psoralen and 5-MOP.

The bond lengths and atomic spin densities in the psoralen skeletons of the furan monoadducts are summarized in Tables 4 and 5, respectively. Because the C4′–C5′ double

Table 1. Bond Distances in Isolated Psoralen, 5-MOP, and 8-MOP Molecules in the S_0 and T_1 States (in Å)

	Psoralen			5-MOP			8-MOP	
	S_0 [a]	T_1^{closed} [b]	T_1^{open} [c]	S_0 [a]	T_1^{closed} [b]	T_1^{open} [c]	S_0 [a]	T_1^{open} [c]
O1–C2	1.400	1.412 (+0.012)	2.219 (+0.819)	1.403	1.409 (+0.006)	2.222 (+0.819)	1.396	2.215 (+0.819)
C2–C3	1.460	1.419 (−0.041)	1.357 (−0.103)	1.457	1.425 (−0.032)	1.354 (−0.103)	1.461	1.356 (−0.105)
C3–C4	1.353	1.458 (+0.105)	1.416 (+0.063)	1.355	1.457 (+0.102)	1.420 (+0.065)	1.353	1.418 (+0.065)
C4–C10	1.443	1.386 (−0.057)	1.425 (−0.018)	1.440	1.383 (−0.057)	1.420 (−0.020)	1.444	1.424 (−0.020)
C10–C9	1.422	1.469 (+0.047)	1.487 (+0.065)	1.418	1.454 (+0.036)	1.471 (+0.053)	1.416	1.477 (+0.061)
C9–O1	1.366	1.366 (0.000)	1.257 (−0.109)	1.363	1.370 (+0.007)	1.257 (−0.106)	1.366	1.256 (−0.110)
C2–O2″	1.204	1.222 (+0.018)	1.167 (−0.037)	1.205	1.218 (+0.013)	1.169 (−0.036)	1.205	1.168 (−0.037)
C10–C5	1.405	1.440 (+0.035)	1.394 (−0.011)	1.419	1.464 (+0.045)	1.410 (−0.009)	1.404	1.394 (−0.010)
C5–C6	1.395	1.387 (−0.008)	1.433 (+0.038)	1.408	1.408 (0.000)	1.449 (+0.041)	1.393	1.430 (+0.037)
C6–C7	1.416	1.423 (+0.007)	1.413 (−0.003)	1.421	1.411 (−0.010)	1.417 (−0.004)	1.417	1.401 (−0.016)
C7–C8	1.388	1.400 (+0.012)	1.379 (−0.009)	1.387	1.412 (+0.025)	1.387 (0.000)	1.401	1.408 (+0.007)
C8–C9	1.395	1.382 (−0.013)	1.446 (+0.051)	1.393	1.372 (−0.021)	1.448 (+0.055)	1.412	1.465 (+0.053)
C7–O1′	1.363	1.360 (−0.003)	1.376 (+0.013)	1.363	1.359 (−0.004)	1.375 (+0.012)	1.373	1.378 (+0.005)
C6–C4′	1.447	1.448 (+0.001)	1.420 (−0.027)	1.456	1.445 (−0.011)	1.427 (−0.029)	1.447	1.429 (−0.018)
C4′–C5′	1.356	1.357 (+0.001)	1.380 (+0.024)	1.354	1.357 (+0.003)	1.379 (+0.025)	1.354	1.370 (+0.016)
C5′–O1′	1.379	1.382 (+0.003)	1.358 (−0.021)	1.375	1.374 (−0.001)	1.352 (−0.023)	1.376	1.363 (−0.013)
$C5–O_{methoxy}$				1.359	1.353 (−0.006)	1.363 (+0.004)		
$C8–O_{methoxy}$							1.352	1.336 (−0.016)
$O_{methoxy}–C_{methoxy}$				1.422	1.423 (+0.001)	1.418 (−0.004)	1.428	1.431 (+0.003)

a) Bond distances in the ground-state structure. b) Bond distances in the closed-ring structure in the T_1 state. Differences from the bond distances in the ground-state structure are shown in parentheses. c) Bond distances in the open-ring structure in the T_1 state. Differences from the bond distances in the ground-state structure are shown in parentheses.

Table 2. Atomic Spin Densities of Isolated Psoralen, 5-MOP, and 8-MOP Molecules in the S_0 and T_1 States

	Psoralen			5-MOP			8-MOP	
	S_0 [a]	T_1^{closed} [b]	T_1^{open} [c]	S_0 [a]	T_1^{closed} [b]	T_1^{open} [c]	S_0 [a]	T_1^{open} [c]
O1	+0.075	+0.053	+0.296	+0.012	+0.034	+0.274	+0.077	+0.287
C2	−0.010	−0.052	+0.168	−0.003	−0.049	+0.162	+0.024	+0.167
O2″	+0.308	+0.332	+0.125	+0.137	+0.253	+0.110	+0.097	+0.118
C3	+0.536	+0.638	−0.004	+0.487	+0.665	−0.024	+0.167	−0.014
C4	+0.369	+0.414	+0.481	+0.215	+0.383	+0.491	+0.093	+0.493
C5	+0.197	+0.267	+0.265	+0.455	+0.340	+0.254	+0.641	+0.306
C6	+0.026	−0.035	+0.184	−0.072	−0.107	+0.198	+0.037	+0.122
C7	+0.257	+0.267	−0.008	+0.134	+0.224	−0.022	−0.005	−0.008
C8	−0.085	−0.106	+0.329	+0.270	−0.012	+0.397	+0.350	+0.300
C9	+0.188	+0.186	+0.002	−0.083	+0.086	−0.007	+0.114	+0.048
C10	+0.123	+0.050	−0.025	+0.188	+0.089	−0.088	−0.014	−0.064
O1′	−0.009	+0.004	+0.017	+0.052	+0.029	+0.029	+0.045	+0.035
C4′	−0.019	+0.006	−0.028	+0.081	+0.058	−0.018	+0.076	−0.015
C5′	+0.098	+0.035	+0.259	+0.030	−0.035	+0.247	+0.200	+0.159
$O_{methoxy}$				+0.136	+0.086	+0.048	+0.144	+0.109
$C_{methoxy}$				−0.010	−0.006	−0.004	−0.010	−0.008

a) Atomic spin densities in the ground-state structure. b) Atomic spin densities in the closed-ring structure in the T_1 state. c) Atomic spin densities in the open-ring structure in the T_1 state.

bond forms a ring with the C5–C6 bond of thymine, the C4′–C5′ bonds were elongated to about 1.56 Å. In the closed-ring structures, the C3–C4 bonds were elongated by about 0.1 Å, and the spin densities at C3 and C4 were about 0.64 and 0.35, respectively. The large bond elongations and spin distribution at C3–C4 sites imply that the C3–C4 bond is reactive.

In the open-ring structures, the O1–C2 distances were more than 2.2 Å. The bond elongations of the C3–C4 bond are about 0.06 Å, which are smaller than those in the closed-ring structures. Only C4 had large spin density in the open-ring structure while both C3 and C4 had large spin densities in the closed-ring structure: the absolute values of the spin densities at C4 were about 0.5 while those at C3 were at most 0.04. These bond distances and spin distribution suggest that the activity of the C3–C4 site decreases in the open-ring structure. The trend in the differences in the spin distribution between the closed- and open-ring structures in the furan monoadducts is similar to that in the isolated systems. Therefore, it is indicated that 8-MOP, which has stable open-ring structure in both the isolated system and the furan monoadduct, is less likely to lead

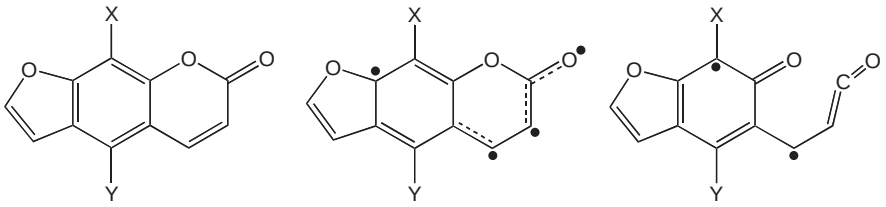

Fig. 3. Bond arrangement in the closed- and open-ring structures in the T_1 states.

Table 3. Stabilization Energies of 5-MOP and 8-MOP Isomers in the T_1 States (in eV)

	T_1^{closed} a)	T_1^{open} b)
5-MOP isomer	0.59	0.48
8-MOP isomer	0.39	0.38

a) Stabilization energies of the closed-ring structure in the T_1 state. b) Stabilization energies of the open-ring structure in the T_1 state.

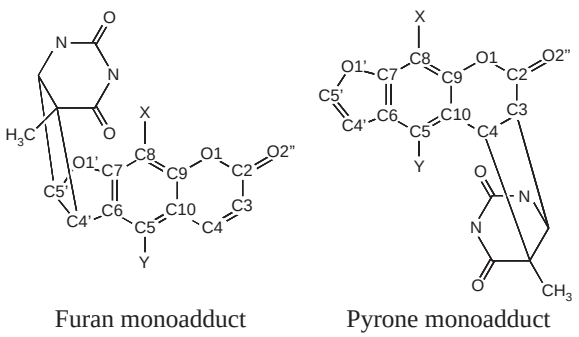

Fig. 4. Chemical structures of furan and pyrone monoadducts of psoralens. The numbering in this figure (O1, C2, O2″, C3, C4, C5, C6, C7, C8, C9, C10, O1′, C4′, and C5′) corresponds to IUPAC numbering (O8, C7, O7′, C6, C5, C4, C3a, C9a, C9, C8a, C4a, O1, C2, and C3).

to the undesirable cross-linking DNA than psoralen and 5-MOP are.

Designs of the Monofunctional Psoralen Compounds. Based on the results in the previous two sections, the psoralen compound having a stable open-ring structure in the T_1 state is expected to be a monofunctional psoralen. Investigating what kind of psoralen compound has a stable open-ring structure is important, because monofunctional psoralen has a low risk of side effects. Therefore, the stabilization energies of 20 kinds of substituted psoralens were calculated in order to investigate the substituent effect on the stability of the open-ring structure.

Table 6 summarizes the stabilization energies of the substituted psoralen compounds: 14 compounds with the substituent X (X = OCH_2CH_3, NH_2, $OCH_2CH_2CH_3$, OH, SH, SCH_3, OCF_3, CHO, F, CN, COOH, CH_3, CF_3, and NO_2) at the 8-position (8-X), five compounds with Y (Y = CH_3, OH, OCH_2CH_3, NO_2, and CN) at the 5-position (5-Y), and 5,8-dimethoxypsoralen, in which the methoxy groups are at both the 5- and 8-positions (8-X–5-Y; X = Y = OCH_3). The stabiliza-

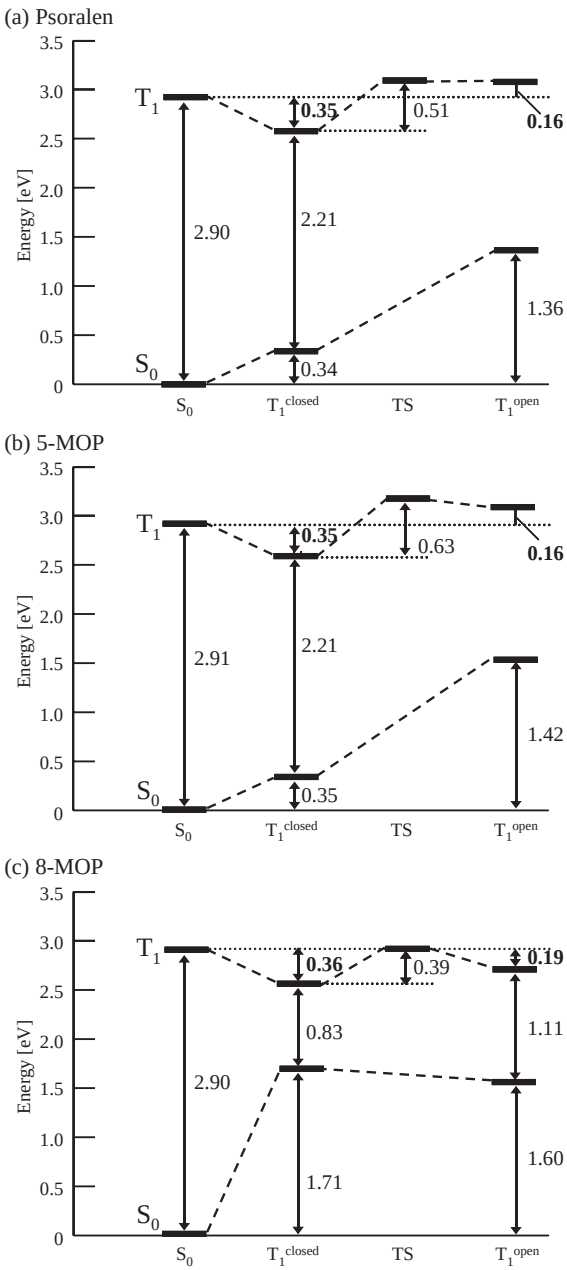

Fig. 5. Energy diagrams in the S_0 and T_1 states for the furan monoadducts of (a) psoralen, (b) 5-MOP, and (c) 8-MOP. Stabilization energies from the T_1-state energies at the ground-state structures are shown in boldface.

Table 4. Bond Distances in the Psoralen Skeletons in the Furan Monoadducts of Psoralen, 5-MOP, and 8-MOP in the S_0 and T_1 States (in Å)

	Psoralen			5-MOP			8-MOP		
	S_0 [a]	T_1^{closed} [b]	T_1^{open} [c]	S_0 [a]	T_1^{closed} [b]	T_1^{open} [c]	S_0 [a]	T_1^{closed} [b]	T_1^{open} [c]
O1–C2	1.408	1.417 (+0.009)	2.234 (+0.826)	1.411	1.413 (+0.002)	2.255 (+0.844)	1.408	1.415 (+0.007)	2.328 (+0.920)
C2–C3	1.457	1.422 (−0.035)	1.360 (−0.097)	1.454	1.425 (−0.029)	1.358 (−0.096)	1.457	1.426 (−0.031)	1.350 (−0.107)
C3–C4	1.356	1.452 (+0.096)	1.412 (+0.056)	1.357	1.454 (+0.097)	1.414 (+0.057)	1.356	1.452 (+0.096)	1.422 (+0.066)
C4–C10	1.439	1.383 (−0.056)	1.437 (−0.002)	1.437	1.383 (−0.054)	1.437 (0.000)	1.440	1.383 (−0.057)	1.424 (−0.016)
C10–C9	1.415	1.464 (+0.049)	1.481 (+0.066)	1.410	1.453 (+0.043)	1.478 (+0.068)	1.415	1.460 (+0.045)	1.472 (+0.057)
C9–O1	1.359	1.365 (+0.006)	1.262 (−0.097)	1.358	1.369 (+0.011)	1.262 (−0.096)	1.361	1.370 (+0.009)	1.264 (−0.097)
C2–O2″	1.204	1.219 (+0.015)	1.167 (−0.037)	1.204	1.218 (+0.014)	1.168 (−0.036)	1.204	1.218 (+0.014)	1.168 (−0.036)
C10–C5	1.413	1.448 (+0.035)	1.395 (−0.018)	1.429	1.468 (+0.039)	1.400 (−0.029)	1.412	1.450 (+0.038)	1.399 (−0.013)
C5–C6	1.383	1.373 (−0.010)	1.415 (+0.032)	1.398	1.388 (−0.010)	1.421 (+0.023)	1.383	1.371 (−0.012)	1.420 (+0.037)
C6–C7	1.410	1.418 (+0.008)	1.408 (−0.002)	1.416	1.419 (+0.003)	1.406 (−0.010)	1.407	1.416 (+0.009)	1.375 (−0.032)
C7–C8	1.387	1.402 (+0.015)	1.378 (−0.009)	1.383	1.401 (+0.018)	1.376 (−0.007)	1.395	1.416 (+0.021)	1.422 (+0.027)
C8–C9	1.401	1.383 (−0.018)	1.441 (+0.040)	1.399	1.379 (−0.020)	1.445 (+0.046)	1.411	1.390 (−0.021)	1.460 (+0.049)
C7–O1′	1.366	1.367 (+0.001)	1.376 (+0.010)	1.368	1.366 (−0.002)	1.377 (+0.009)	1.366	1.361 (−0.005)	1.373 (+0.007)
C6–C4′	1.508	1.507 (−0.001)	1.499 (−0.009)	1.514	1.514 (0.000)	1.493 (−0.021)	1.508	1.506 (−0.002)	1.507 (−0.001)
C4′–C5′	1.557	1.555 (−0.002)	1.557 (0.000)	1.555	1.555 (0.000)	1.557 (+0.002)	1.557	1.555 (−0.002)	1.560 (+0.003)
C5′–O1′	1.435	1.435 (0.000)	1.431 (−0.004)	1.434	1.433 (−0.001)	1.441 (+0.007)	1.435	1.436 (+0.001)	1.436 (+0.001)
$C5–O_{methoxy}$				1.355	1.352 (−0.003)	1.372 (+0.017)	1.362	1.361 (−0.001)	1.331 (−0.031)
$C8–O_{methoxy}$									
$O_{methoxy}–C_{methoxy}$				1.428	1.427 (−0.001)	1.444 (+0.016)	1.440	1.440 (0.000)	1.442 (+0.002)

a) Bond distances in the ground-state structure. b) Bond distances in the closed-ring structure in the T_1 state. Differences from the bond distances in the ground-state structure are shown in parentheses. c) Bond distances in the open-ring structure in the T_1 state. Differences from the bond distances in the ground-state structure are shown in parentheses.

Table 5. Atomic Spin Densities of the Furan Monoadducts of Psoralen, 5-MOP, and 8-MOP in the T_1 States

	Psoralen		5-MOP		8-MOP	
	T_1^{closed} [a]	T_1^{open} [b]	T_1^{closed} [a]	T_1^{open} [b]	T_1^{closed} [a]	T_1^{open} [b]
O1	+0.056	+0.342	+0.053	+0.345	+0.052	+0.344
C2	−0.050	+0.188	−0.051	+0.189	−0.048	+0.177
O2″	+0.294	+0.153	+0.269	+0.145	+0.272	+0.111
C3	+0.633	+0.033	+0.655	+0.016	+0.637	−0.040
C4	+0.354	+0.499	+0.367	+0.513	+0.345	+0.518
C5	+0.206	+0.087	+0.196	+0.081	+0.225	+0.264
C6	−0.020	+0.364	−0.097	+0.376	−0.043	+0.112
C7	+0.295	−0.014	+0.305	−0.023	+0.319	+0.073
C8	−0.104	+0.211	−0.076	+0.239	−0.083	+0.306
C9	+0.193	−0.001	+0.182	−0.002	+0.177	+0.053
C10	+0.090	+0.141	+0.110	+0.111	+0.092	−0.075
O1′	+0.092	+0.013	+0.079	+0.009	+0.103	+0.023
C4′	−0.002	−0.028	+0.005	−0.031	−0.000	−0.008
C5′	−0.006	+0.002	−0.006	+0.005	−0.007	−0.001
$O_{methoxy}$			+0.046	+0.002	−0.001	+0.152
$C_{methoxy}$			−0.004	+0.010	−0.002	−0.008

a) Atomic spin densities in the closed-ring structure in the T_1 state. b) Atomic spin densities in the open-ring structure in the T_1 state.

tion energies of psoralen (8-H–5-H), 5-MOP (5-OCH_3), and 8-MOP (8-OCH_3) are again shown in Table 6. The energy differences between the closed- and open-ring structures are shown in parentheses, which correspond to the relative stabilities of the closed- and open-ring structures, and the positive values mean that the open-ring structures are more stable than the closed-ring ones. Hammett constants (σ_p), which reflect the electron-donating abilities of the substituents, are also shown in Table 6. In particular, σ_R reflects the resonance effect of the substituent. A negative value of σ_p (σ_R) implies the electron-donating (electron-donating resonance) character of the substituent.[25]

Addition of an electron-donating group at the 8-position leads to the cleavage of the O1–C2 bond. For 8-X with X = OCH_2CH_3, OCH_3 (8-MOP), NH_2, and $OCH_2CH_2CH_3$, only the open-ring structure was obtained as a stationary point in the T_1 state. The OCH_2CH_3, OCH_3, NH_2, and $OCH_2CH_2CH_3$ groups are strong electron-donating groups, having especially

Table 6. Stabilization Energies of the Substituted Psoralen Compounds in the T_1 States (in kcal mol^{-1})

	Substituent				Stabilization energy		
	X	Y	σ_p [a]	σ_R [a]	T_1^{closed} [b]	T_1^{open} [c]	$\Delta(T_1^{open} - T_1^{closed})$ [d]
8-X	OCH_2CH_3	H	−0.24	−0.44	—	12.22	—
	OCH_3	H (8-MOP)	−0.27	−0.43	—	10.98	—
	NH_2	H	−0.66	−0.48	—	10.85	—
	$OCH_2CH_2CH_3$	H	—	—	—	10.79	—
	OH	H	−0.37	−0.43	9.32	11.72	2.40
	SH	H	0.15	−0.15	8.71	10.71	1.99
	SCH_3	H	0.00	−0.17	8.48	9.66	1.18
	OCF_3	H	0.35	−0.04	9.21	10.35	1.14
	CHO	H	0.42	0.24	7.37	7.88	0.50
	F	H	0.06	−0.34	9.25	9.34	0.09
	CN	H	0.66	0.13	8.96	8.95	−0.01
	COOH	H	0.45	0.29	7.78	7.19	−0.59
	CH_3	H	−0.17	−0.11	8.54	7.48	−1.06
	CF_3	H	0.54	0.10	8.66	6.80	−1.86
	NO_2	H	0.78	0.15	7.50	5.61	−1.89
5-Y	H	CH_3	−0.17	−0.11	8.61	4.62	−4.00
	H	OH	−0.37	−0.43	9.04	4.65	−4.39
	H	OCH_3 (5-MOP)	−0.27	−0.43	9.16	3.04	−6.13
	H	OCH_2CH_3	−0.24	−0.44	8.59	2.45	−6.14
	H	NO_2	0.78	0.15	7.21	—	—
	H	CN	0.66	0.13	8.54	—	—
8-X–5-Y	OCH_3	OCH_3	−0.27	−0.43	7.82	5.87	−1.95
	H	H (Psoralen)	—	—	8.55	5.63	−2.92

a) Reference 25. b) Stabilization energies of the closed-ring structure in the T_1 state. c) Stabilization energies of the open-ring structure in the T_1 state. d) Energy differences between the closed- and open-ring structures in the T_1 state.

π-electron donating resonance effects. As for 8-X with X = OH, SH, SCH_3, OCF_3, and CHO, both the closed- and open-ring structures were obtained, and the open-ring structure was more stable than the closed-ring structure. The closed-ring structure was as stable as the open-ring one for 8-F and 8-CN: the energy differences were less than 0.1 kcal mol^{-1}. For 8-X with X = COOH, CF_3, and NO_2, which are electron-withdrawing substituents, the closed-ring structures were more stable than the open-ring ones. It should be noted that the closed-ring structure was more stable than the open-ring structure for 8-CH_3, although CH_3 is an electron-donating group.

For all 5-Y and 8-X–5-Y molecules, the closed-ring structures are more stable than the open-ring structures. For 5-Y compounds with Y = CH_3, OH, OCH_3 (5-MOP), and OCH_2-CH_3, the energy differences between the closed- and open-ring structures were about or more than 4 kcal mol^{-1}. Only the closed-ring structures were found for 5-Y with Y = NO_2 and CN, which are strong electron-withdrawing substituents. The energy difference between the closed- and open-ring structures of 8-OCH_3–5-OCH_3 was smaller than that in 5-MOP, which indicates that the substituent effects of the methoxy groups at the 5- and 8-positions cancel out each other in 8-OCH_3–5-OCH_3.

Figure 6 plots the stabilization energies of (a) the closed-ring structures, (b) the open-ring structures, and (c) the energy differences between the closed- and open-ring structures versus σ_p and σ_R. Figure 6a shows that the stability of the closed-ring structure depends little on the electron-donating ability of the substituent: most of the plots are distributed in the range of 7–10 kcal mol^{-1}. Both for 8-X and 5-Y, the closed-ring structure becomes more stable when the substituent at the 5- or 8-positions has strong electron-donating ability.

On the other hand, the stability of the open-ring structure strongly depends on the electron-donating ability of the substituent. In Fig. 6b, the plots are widely distributed over the range of 2–13 kcal mol^{-1}. In particular, the stabilization energies of the open-ring structures of 8-X were larger than those of 5-Y; the plots of 8-X are distributed over the range of 5–13 kcal mol^{-1} while those of 5-Y are in the range of 2–5 kcal mol^{-1}. It was found for 8-X, but not for 5-Y, that the stabilization energy of the open-ring structure increased as the electron-donating ability of the substituent increases.

Figure 6c shows the relationship between the electron-donating abilities of the substituents and the relative stabilities of the closed- and open-ring structures. σ_p and σ_R are the abscissas in Figs. 6c(1) and 6c(2), respectively, so that Fig. 6c(2) focuses on the resonance effect of the substituent. The behavior of the distributions of the plots in Figs. 6c(1) and 6c(2) are closer to that in Fig. 6b than that in Fig. 6a, which indicates that the relative stabilities of the closed- and open-ring structures depend on the stability of the open-ring structure more strongly than on that of the closed-ring structure. All of the compounds above the horizontal axis, for which the open-ring structures were more stable than the closed-ring structures, correspond to 8-X compounds. Furthermore, in Fig. 6c(2), most of the plots above the horizontal axis are distributed

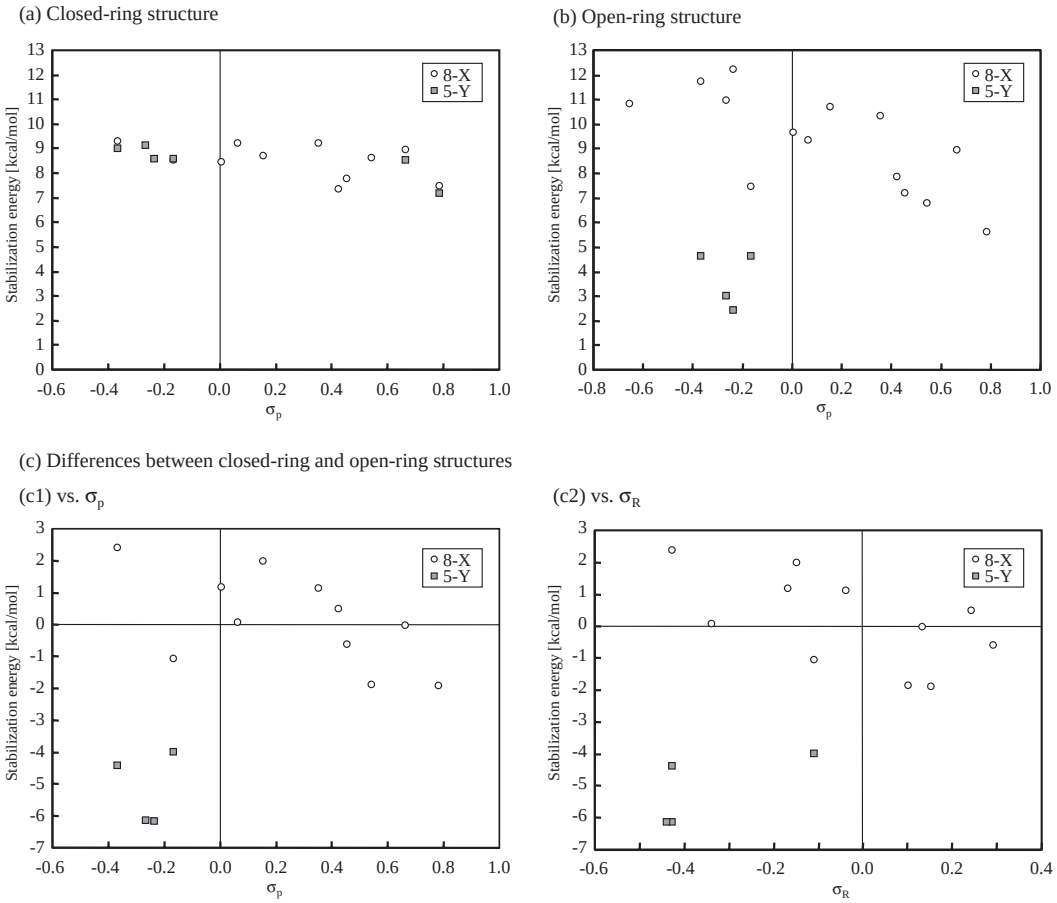

Fig. 6. Correlation between Hammett constants and the stabilization energies of (a) the closed-ring structures, (b) the open-ring structures, and (c) the energy differences between the closed- and open-ring structures.

in the second quadrant. It suggests that the stability of the open-ring structure depends on the position and the electron-donating resonance effect of the substituent. Therefore, it is concluded that the substitution of an electron-donating group with strong electron-donating resonance effect at the 8-position of psoralen gives a monofunctional compound, which leads to no harmful diadduct.

Conclusion

In the present theoretical study, the stable ring-opening structure in the T_1 state, in which the pyrone ring is cleaved, was studied. The bond distances and spin densities in the open-ring structure indicate that the activity of the C3–C4 bond decreases in the open-ring structure. In particular, only the open-ring structure was obtained for 8-MOP, whereas both the closed- and open-ring structures were obtained for psoralen and 5-MOP. The stability of the open-ring structures of 8-MOP was demonstrated also in the case of furan monoadducts. Based on these results, it is suggested that the 8-MOP is less likely to lead to undesirable cross-linking DNA than psoralen and 5-MOP are. Furthermore, the dependence of the stability of the open-ring structure on the position and the electron-donating nature of the substituents was investigated. It was found that the psoralen compound having an electron-donating substituent at the 8-position tended to have a stable open-ring structure and should expected to be a monofunctional psoralen.

We acknowledge Professor H. Takahashi for valuable discussions. We would like to thank Dr. Y. Kawamura and Dr. K. Sodeyama for giving advice on the present calculations. The calculations were performed in part at the Research Center for Computational Science (RCCS) of the Okazaki National Research Institutes. This work was supported by a Grant-in-Aid for Scientific Research on Priority Areas “Molecular Theory for Real Systems” “KAKENHI 18066016” from Japanese Ministry of Education, Culture, Sports, Science and Technology (MEXT), the Next Generation Super Computing Project, Nanoscience Program, of MEXT, and a project research grant “Development of high-performance computational environment for quantum chemical calculation and its assessment” from the Advanced Research Institute for Science and Engineering (RISE) of Waseda University. One of the authors (A.N.) is indebted to the Japanese Society for the Promotion of Science (JSPS) Research Fellowship for Young Scientists.

References

1 T. Otsuki, *J. Synth. Org. Chem., Jpn.* **1991**, *49*, 809.

2 R. V. Bensasson, E. J. Land, T. G. Truscott, *Excited States and Free Radicals in Biology and Medicine*, Oxford University Press, New York, **1993**.

3 P. S. Song, K. J. Tapley, Jr., *Photochem. Photobiol.* **1979**,

29, 1177.

4 Y. Uesugi, H. Takahashi, Symposium on Structure Dynamics and Control of Excited States, Hawaii, **1995**.

5 H. Nakai, Y. Yamauchi, A. Nakata, T. Baba, H. Takahashi, *J. Chem. Phys.* **2003**, *119*, 4223.

6 J. J. Serrano-Pérez, L. Serrano-Andrés, M. Merchán, *J. Chem. Phys.* **2006**, *124*, 124502.

7 J. Tatchen, M. Kleinschmidt, C. M. Marian, *J. Photochem. Photobiol., A* **2004**, *167*, 201.

8 C. M. Estévetz, A. M. Graña, M. A. Ríos, J. Rodríguez, *THEOCHEM* **1991**, *231*, 163.

9 R. Boggia, M. Fanciullo, L. Finzi, O. Incani, L. Mosti, *Il Farmaco* **1999**, *54*, 202.

10 A. D. S. Marques, Y. Takahata, J. R. L. Junior, M. C. Souza, S. S. Simoes, W. M. Azevedo, G. F. de Sa, *J. Lumin.* **2002**, *97*, 237.

11 J. Tatchen, C. M. Marian, *Phys. Chem. Chem. Phys.* **2006**, *8*, 2133.

12 J. J. Serrano-Pérez, M. Merchán, L. Serrano-Andrés, *Chem. Phys. Lett.* **2007**, *434*, 107.

13 A. Nakata, T. Baba, H. Takahashi, H. Nakai, *J. Comput. Chem.* **2004**, *25*, 179.

14 H. P. Spielmann, T. J. Dwyer, J. E. Hearst, D. E. Wemmer, *Biochemistry* **1995**, *34*, 12937.

15 D. Kanne, K. Straub, H. Rapoport, J. E. Hearst, *Biochemistry* **1982**, *21*, 861.

16 A. D. Becke, *J. Chem. Phys.* **1993**, *98*, 5648.

17 P. J. Stephens, F. J. Devlin, C. F. Chabalowski, M. J. Frisch, *J. Phys. Chem.* **1994**, *98*, 11623.

18 J. C. Slater, *Phys. Rev.* **1951**, *81*, 385.

19 A. D. Becke, *Phys. Rev. A* **1988**, *38*, 3098.

20 S. H. Vosko, L. Wilk, M. Nusair, *Can. J. Phys.* **1980**, *58*, 1200.

21 C. Lee, W. Yang, R. G. Parr, *Phys. Rev. B* **1988**, *37*, 785.

22 T. H. Dunning, Jr., *J. Chem. Phys.* **1989**, *90*, 1007.

23 H. Matsumoto, Y. Ohkura, *Chem. Pharm. Bull.* **1978**, *26*, 3433.

24 M. J. Frisch, G. W. Trucks, H. B. Schlegel, G. E. Scuseria, M. A. Robb, J. R. Cheeseman, J. A. Montgomery, Jr., T. Vreven, K. N. Kudin, J. C. Burant, J. M. Millam, S. S. Iyengar, J. Tomasi, V. Barone, B. Mennucci, M. Cossi, G. Scalmani, N. Rega, G. A. Petersson, H. Nakatsuji, M. Hada, M. Ehara, K. Toyota, R. Fukuda, J. Hasegawa, M. Ishida, T. Nakajima, Y. Honda, O. Kitao, H. Nakai, M. Klene, X. Li, J. E. Knox, H. P. Hratchian, J. B. Cross, V. Bakken, C. Adamo, J. Jaramillo, R. Gomperts, R. E. Stratmann, O. Yazyev, A. J. Austin, R. Cammi, C. Pomelli, J. W. Ochterski, P. Y. Ayala, K. Morokuma, G. A. Voth, P. Salvador, J. J. Dannenberg, V. G. Zakrzewski, S. Dapprich, A. D. Daniels, M. C. Strain, O. Farkas, D. K. Malick, A. D. Rabuck, K. Raghavachari, J. B. Foresman, J. V. Ortiz, Q. Cui, A. G. Baboul, S. Clifford, J. Cioslowski, B. B. Stefanov, G. Liu, A. Liashenko, P. Piskorz, I. Komaromi, R. L. Martin, D. J. Fox, T. Keith, M. A. Al-Laham, C. Y. Peng, A. Nanayakkara, M. Challacombe, P. M. W. Gill, B. Johnson, W. Chen, M. W. Wong, C. Gonzalez, J. A. Pople, *Gaussian 03, Revision C.02*, Gaussian, Inc., Wallingford CT, **2004**.

25 S. L. Murov, L. Carmichael, G. L. Hug, *Handbook of Photochemistry*, 2nd ed., Marcel Dekker, Inc., New York, **1993**.